Interaction of the 47-kDa Talin Fragment and the 32-kDa Vinculin Fragment with Acidic Phospholipids: A Computer Analysis

Markus Tempel,* Wolfgang H. Goldmann,*‡ Gerhard Isenberg,* and Erich Sackmann*
*Department of Biophysics, Technical University of Munich, D-85747 Garching, Germany, and ‡Massachusetts General Hospital, Harvard Medical School, Charlestown, Massachusetts USA

ABSTRACT In recent in vitro experiments, it has been demonstrated that the 47-kDa fragment of the talin molecule and the 32-kDa fragment of the vinculin molecule interact with acidic phospholipids. By using a computer analysis method, we determined the hydrophobic and amphipathic stretches of these fragments and, by applying a purpose-written matrix method, we ascertained the molecular amphipathic structure of α-helices. Calculations for the 47-kDa mouse talin fragment (residues 1-433; NH_2-terminal region) suggest specific interactions of residues 21-39, 287-342, and 385-406 with acidic phospholipids and a general lipid-binding domain for mouse talin (primary amino acid sequence 385-401) and for *Dictyostelium* talin (primary amino acid sequence 348-364). Calculations for the 32-kDa chicken embryo vinculin fragment (residues 858-1066; COOH-terminal region) and from nematode vinculin alignment indicate for chicken embryo vinculin residues 935-978 and 1020-1040 interactions with acidic phospholipids. Experimental confirmation has been given for vinculin (residues 916-970), and future detailed experimental analyses are now needed to support the remaining computational data.

INTRODUCTION

One of the most thoroughly studied and possibly the most complicated connection between actin and the cell membrane is the complex of proteins and lipids that form at sites where cells attach to the extracellular matrix. The transmembrane proteins of the integrin family were first thought to be responsible for linking the actin cytoskeleton to the lipid membrane, but the order with which other proteins bind integrins, lipids, actin, or each other is only partly understood and is still under investigation (Isenberg, 1991). The major protein components that assemble at sites of attachment of the cell to extracellular matrix are vinculin, talin, and α-actinin (Otto, 1990; Beckerle and Yeh, 1990). These proteins are believed to form, with each other and with other components, complexes that serve to link filamentous actin to the membrane. Their molecular interactions are best understood in focal contacts (or adhesion plaques), i.e., specialized membrane regions for the attachment of cells to the extracellular matrix. In addition to these relatively abundant components, other proteins are found preferentially associated with these structures. These proteins include tensin, zyxin, ezrin, filamin, and paxillin (Pavalko et al., 1991; Turner et al., 1990; Geiger and Ginsberg, 1991). These less abundant proteins may be responsible, in part, for regulation of the larger focal contact complexes. For example, zyxin binds to the NH_2-terminal 27-kDa domain of α-actinin, which also contains the actin binding site (Crawford et al., 1992). This interaction could be involved in coordinating actin organization and membrane attachment. Other possible regulatory mechanisms include integrin, vinculin, and paxillin tyrosine phosphorylation by pp60-src (Sefton and Hunter, 1981; Maher et al., 1985; Glenney and Zokas, 1989).

Talin binds in vitro vinculin (Burridge and Mangeat, 1984) and α-actinin (Wachsstock et al., 1987), interacts with actin (Goldmann and Isenberg, 1991), promotes actin nucleation (Kaufmann et al., 1991), and induces an increase in internal F-actin chain stiffness (Ruddies et al., 1993) and a decrease in actin filament dynamics (Goldmann et al., 1993). Furthermore, talin is capable of interacting with phospholipid membranes. This interaction may be mediated by a linkage to the cytoplasmic domains of integrins (Horwitz et al., 1986) or by direct binding to acidic phospholipids. The lipid-binding activity of the talin molecule has been demonstrated in vitro by various techniques on lipid mono- and bilayers, such as differential scanning calorimetry in combination with Fourier transformed infrared spectroscopy (Heise et al., 1991), hydrophobic photolabeling (Goldmann et al., 1992), fluorescence light microscopy (Kaufmann et al., 1992), and film balance technique (Dietrich et al., 1993). The incorporation rate of talin into zwitterionic phospholipid bilayers (PC) is low although greatly enhanced in the presence of negatively charged phospholipids (PG and PS).

Vinculin binds in vitro talin (see above), α-actinin (Belkin and Koteliansky, 1987), paxillin (Turner et al., 1990; Wood et al., 1994), actin (Jockusch and Isenberg, 1981), and itself (Johnson and Craig, 1994) and shows only little influence on internal actin filament dynamics (Götter et al., 1995). Furthermore, the vinculin molecule inserts into the hydrophobic core of mono- and bilayers as shown in vitro

Received for publication 8 December 1994 and in final form 4 April 1995.
Address reprint requests to Dr. Markus Tempel, Technical University of Munich, Biophysics, E22, James Franck St., D-85747 Garching, Germany. Tel. 011-49-89-3209-2477; Fax: 011-49-89-3209-2469; E-mail: mtempel@physik. tu-muenchen.de.

Abbreviations used: PC, phosphatidylcholine; PG, phosphatidylglycerol; PS, phosphatidylserine; PA, phosphatidylacid; PI, phosphatidylinositol; PE, phosphatidylethanolamine; SDS-PAGE, sodium dodecyl sulfate polyacrylamide gel electrophoresis; GCG, Genetic Computer Group; pI, isoelectric point.

0006-3495/95/07/228/14 $2.00

by the film balance technique (Fringeli et al., 1986; Meyer, 1989) and in labeling experiments (Ito et al., 1983; Niggli et al., 1986; Goldmann et al., 1992). A specifity exists for acidic phospholipids (PA, PI, and PG) whereas neutral lipids (PC and PE) do not promote binding. A vinculin-bilayer association also occurs in chicken embryo fibroblasts incubated with photoactivatable fatty acids (Niggli et al., 1990).

Human platelet talin in its biologically active state is a dumbbell-shaped homodimer of ~51 nm length (Goldmann et al., 1994). Rotary-shadowed-electron microscopy revealed two antiparallel associated talin monomers, each molecule with a globular head domain and a rod-like tail domain. Judging from SDS-PAGE, talin has a molecular mass of ~225 kDa (Beckerle et al., 1986). Talin can be cleaved by calpain II into a head fragment of ~47 kDa and into a tail fragment of ~200 kDa. The primary amino acid sequence of mouse talin has a total of 2541 residues, with the calpain II cleavage site located between residues 433 and 434. The NH_2-terminal region (residues 1-433) with a calculated molecular mass of ~50 kDa corresponds to the ~47-kDa fragment, whereas the heavy ~200-kDa fragment is assigned to the COOH-terminal region (residues 434-2541) with a calculated molecular mass of ~220 kDa (Rees et al., 1990). Computer Fourier analysis of the COOH-terminal primary sequence (residues 434-2541) showed a weak pattern of repetitive α-helical motifs, suggesting an elongated, rod-like tail (McLachlan et al., 1994). The 200-kDa talin tail fragment shows binding sites for vinculin (Gilmore et al., 1993) and integrins (Simon and Burridge, 1991). Computer sequence analysis revealed for the 47-kDa head region homologies with the membrane-binding domains of protein 4.1, ezrin (Rees et al., 1990), and a talin homologue of *Dictyostelium* (Kreitmeier et al., 1995). Niggli and co-workers (1994) have identified in several in vitro experiments with human platelet talin additional functional domains in the 47-kDa and 200-kDa fragments: The 47-kDa fragment interacts specifically with acidic membranes, whereas the 200-kDa fragment is specifically responsible for actin interaction and nucleation. The 47-kDa polypeptide lacks any functional activity with actin but retains the lipid-binding capacity of the intact talin molecule. The specific interaction of the small 47-kDa fragment with acidic membranes was demonstrated by hydrophobic photolabeling, with ^{125}I-labeled PS liposomes and in co-sedimentation measurements, also with PS liposomes (Niggli et al., 1994).

According to the results from rotary-shadowed electron microscope images (Milam, 1985) and dynamic light scattering experiments (Eimer et al., 1993), the molecular shape of isolated vinculin molecules can be described by a balloon-on-a-string model composed of a globular head and an extended, flexible tail. Vinculin is a highly conserved protein with 1066 primary sequence residues in chicken and human (Price et al., 1987, 1989; Coutu and Craig, 1988; Weller et al., 1990) and of a calculated molecular mass of 117 kDa. Judged from SDS-PAGE, the molecular mass is ~130-kDa (Geiger et al., 1980). The globular head domain can be cleaved from the tail domain by V8 protease, which generates on SDS-PAGE fragments of ~90-kDa and ~32-kDa molecular mass (Price et al., 1989). The globular 90-kDa fragment extends over the primary sequence residues 1-857 (Milam, 1985) and is connected to the 32-kDa tail fragment (residues 858-1066) by a flexible hinge, consisting of a proline-rich region (residues 837-878) (Coutu and Craig, 1988). Within residues 1-100 and 1-258 of the NH_2-terminal head fragment, the α-actinin-binding domain (Kroemker et al., 1994) and the talin-binding domain (Jones et al., 1989; Gilmore et al., 1992) are localized, whereas the COOH-terminal tail fragment includes, along the residues 893-1028, the focal contact targeting sequence, the paxillin-binding domain, and the F-actin-binding domain (Wood et al., 1994; Menkel et al., 1994).

Recent studies on chicken gizzard vinculin revealed the existence of a high affinity, intramolecular interaction between the NH_2-terminal head and the COOH-terminal tail domain (Johnson and Craig, 1994). According to Johnson and Craig (1995), this head-tail interaction is capable of modulating the affinity of vinculin to actin. Although the tail fragment alone includes a high affinity binding site for acidic phospholipids, the addition of head fragments to tail fragments inhibits the high affinity site leading to a low affinity lipid interaction. These findings indicate that the globular head domain and the extended tail domain of vinculin molecules have different functions when regulating lipid binding.

The high affinity lipid-binding site(s) of the large proteins talin (225 kDa) and vinculin (130 kDa) are localized in the small cleavage fragments of these proteins, the 47-kDa fragment for talin (Niggli et al., 1994) and the 32-kDa fragment for vinculin (Johnson and Craig, 1992). It was, therefore, intriguing to subject the two comparatively short amino acid regions, mouse talin residues 1-433 and chicken embryo vinculin residues 858-1066, to a detailed computer examination on lipid-binding site(s). For the determination of hydrophobic and amphipathic stretches with high lipid-binding probability, an established method by Eisenberg and co-workers (1984) was used. Furthermore, a new mathematical method based on a matrix for the distribution of physicochemically different amino acids along amphipathic α-helices was introduced and applied. In addition to these computations, secondary structure predictions and charge distribution calculations were carried out.

MATERIALS AND METHODS

Detection of hydrophobic and amphipathic α-helices

Values for the mean hydrophobicity $\langle H \rangle$ and the mean hydrophobic moment $\langle \mu_H \rangle$ were computed according to the procedure of Kyte and Doolittle (1982) and Eisenberg et al. (1982), respectively, with the hydrophobic moment being the hydrophobicity of a peptide calculated for different angles of rotation per residue. This procedure was used as a measure of the probability that the peptide separates hydrophobic and

hydrophilic residues in a periodic structure. Here, the hydrophobic moment was always calculated for the secondary structure α-helix, i.e., a rotation angle of 100° between adjacent residues. A high numerical value of the helical hydrophobic moment indicated an amphipathic helix that was characterized by a polar and a nonpolar helix side. The normalized consensus scale developed by Eisenberg et al. (1984) was taken as the hydrophobicity scale for amino acids.

To detect and to classify the amino acid sequence of talin vinculin segments, which can bind to lipids in a hydrophobic or amphipathic way, the Eisenberg plot was used (Eisenberg et al., 1984). Eisenberg and co-workers plotted the average helical hydrophobic moment $\langle\mu_H\rangle$ against the average hydrophobicity $\langle H\rangle$ for 11-residue-long segments of various proteins and peptides and observed different patterns of globular, surface, and transmembrane segments. (Note that surface segments denote amino acid segments that bind to lipid membranes via an amphipathic helix; the helix axis is directed parallel to the surface of the membrane where the polar helix side interacts with the aqueous phase and/or the lipid headgroups, and the nonpolar helix side interacts with the lipid acyl chains. In this context we also use the term surface-seeking.) According to Eisenberg et al. (1984), the various regions can be roughly divided by boundary lines. The boundaries are defined as follows. (1) Transmembrane α-helices are assumed if the mean hydrophobicity $\langle H\rangle > 0.51$ and the mean hydrophobic moment $\langle\mu_H\rangle \leq 0.603-0.392\ \langle H\rangle$. Within the transmembrane region, helices with a hydrophobic moment $\langle\mu_H\rangle < -0.342+0.600\ \langle H\rangle$ are considered as a monomeric anchor whereas helices in the region above this line are assigned to multimeric helix bundles. (2) Surface helices are thought to exist for $\langle\mu_H\rangle > 0.603-0.392\ \langle H\rangle$ where $\langle H\rangle$ is unrestrained. (3) Helices with $\langle H\rangle \leq 0.51$ and $\langle\mu_H\rangle \leq 0.603-0.392\ \langle H\rangle$ are classified as globular. Transmembrane segments have a low helical hydrophobic moment and a high hydrophobicity. Surface-seeking segments have an average hydrophobicity and a high helical hydrophobic moment.

The detection of transmembrane or surface-seeking regions was achieved by the following method. At a window size of 11, the mean hydrophobicity and mean hydrophobic moment of each 11-residue segment of a protein primary sequence are calculated. To test segments on their transmembrane or surface-seeking propensity, their characteristic $\langle H\rangle$ and $\langle\mu_H\rangle$ values are related to the boundary lines by defining two ratios r_{tm} and $r_{surface}$ for the transition from the globular region to the transmembrane region and the surface-seeking region, respectively:

$$r_{tm} = \langle H\rangle/\langle H\rangle^*$$

$$r_{surface} = \langle\mu_H\rangle/\langle\mu_H\rangle^*\ ,$$

where the boundary values $\langle H\rangle^*$ and $\langle\mu_H\rangle^*$ are 0.51 and $0.603-0.392\ \langle H\rangle$, respectively. Taking into consideration the boundaries of the transmembrane, surface-seeking, and globular regions in the Eisenberg plot (see above), three possibilities for the analysis of the two ratios, r_{tm} and $r_{surface}$, have to be distinguished. (1) If for a segment both ratios are ≤1, then this segment is categorized as globular. (2) If one ratio is >1 and the other ratio is ≤1, the former ratio determines the character of the segment; i.e., a segment with the ratio $r_{tm} > 1$ and $r_{surface} < 1$ is considered as transmembrane segment. (3) If both values, r_{tm} and $r_{surface}$, are >1, then the segment is classified as surface-seeking.

A new mathematical method was applied for the determination of amphipathic helices. This method searches for amphipathic α-helical regions by determining the match between an amino acid segment and a suggested motif. The motif is mathematically defined by a matrix and comprises information about the distribution of physicochemically different amino acids (hydrophobic, polar, positive, negative, and neutral) along the amphipathic structure. The basic idea of this method was taken from the work of Hazelrig et al. (1993). The amphipathic motif defined in this work is based on simple requirements for an effective interaction of an amphipathic α-helix with acidic lipids. The motif is suitable to amino acid segments of length 18 (an ideal α-helix of five loops). However, mathematically there are no restrictions for shorter or longer segments. Arguments for this new method are an unlimited application to different α-helix motifs, a simple mathematical algorithm, and a complete independence of a hydrophobicity scale. The purpose of this method is to support the hydrophobic moment analysis as (1) it is believed to give a better understanding of the molecular structure of amino acid stretches with high hydrophobic moments and (2) allows the detection of amphipathically structured domains that are masked in the hydrophobic moment analysis because of a combination of amino acids with low hydrophobicity index. Detailed descriptions of the method are given in the Appendix.

Detection of charged amino acid regions

The specific binding of talin and vinculin to anionic lipids suggests that the distribution of negatively and positively charged amino acids along these protein sequences play an important role in protein-lipid interactions. To get insight into the arrangement of charged amino acids within protein sequences, a simple mathematical procedure based on linear summation of charges was applied:

$$C = \sum_{i}^{i+n-1} c(i),$$

where C denotes the charge of an n-residue-long segment that extends over the primary amino acid residues i to $i + n - 1$, and $c(i)$ is the charge value of residue i. Positive amino acids (amino acid single letter code K, R, and H) have a charge value of $c = 1$, negative amino acids (E and D) of $c = -1$ and all other amino acids of $c = 0$.

Secondary structure predictions

To obtain a higher confidence level of prediction accuracy, secondary structure predictions were carried out by using the results of four separate predictive methods. These four methods named ALB (Ptitsyn and Finkelstein, 1983), GOR (Garnier et al., 1978; Gibrat et al., 1987), JAMSEK (Mrazek and Kypr, 1988), and SIMPA (Levin and Garnier, 1988) are linked in the program PREDICT of the Genetic Computer Group (GCG) program package (Devereux et al., 1984). Each of the algorithms predicts the α-helix, the β-strand, or the coil for each residue within a sequence. Two of the programs also predict the turn (ALB and JAMSEK). Each of the secondary prediction methods has a prediction accuracy for a single residue between 57 and 63% (SD ± 7% per method). The secondary structure prediction methods should also be considered as a tool to locate positions of specific secondary structures. Identifying the positions of α-helices or β-sheets, the prediction accuracy is ~80%.

To gain a single prediction for each amino acid residue, the results of the four methods were combined by using the following rules. (1) All helix or strand assignments must result from at least four adjoining helical or strand residues. This rule is dominant over the rules 2, 4, and 5. (2) A residue was assigned helical, strand, or coil when three or four methods resulted in the same prediction. (3) When two methods predicted α-helix (or β-strand) and the other methods a combination of coil, β-strand (or α-helix), and turn, then the position was assigned coil. (4) When two methods predicted helical (or β-strand) and the other two methods coil, then the position was assigned helical (or β-strand). (5) When two methods predicted helical and two methods β-strand, then the position was assigned to rule 1. (6) When two methods predicted coil and the other methods a combination of helical, strand, and turn, then the position was assigned coil. (7) When the two methods ALB and JAMSEK predicted turn and the other two methods GOR and SIMPA coil, then the position was assigned turn. (8) When the four methods predicted four different structure types, then the position was assigned coil.

We also used from the GCG program package ISOELECTRIC, an algorithm for the calculation of isoelectric points from protein amino acid compositions, PEPCOIL, a method developed by Lupas et al. (1991) for the determination of α-helical coiled-coil structures in proteins, and BESTFIT, a program to achieve an optimal alignment of the best segment of similarity between two protein sequences.

RESULTS

Validity test of the Eisenberg plot

Helices of transmembrane, surface-seeking, and globular proteins cluster in a plot $\langle\mu_H\rangle$ versus $\langle H\rangle$ in different regions (Eisenberg et al., 1984). According to Eisenberg and coworkers, the various regions can be divided by straight lines. Fig. 1 represents the so-called Eisenberg plot. The boundary lines are drawn for the monomeric/multimeric transmembrane, surface, and globular region. The boundary line between the surface and the globular region was defined by investigating eight surface proteins (cf. Eisenberg et al., 1984). To check this line, calculations were made for an additional 16 lipid-binding proteins of pronounced amphipathic character. These proteins were assigned to protein classes of polypeptide hormones and lytic polypeptides (cf. Segrest et al., 1990). Within each of these short sequences (17–26 residues), the 11-residue segment with the most amphipathic α-helical character was determined and then marked in Fig. 1 with + for polypeptide hormones and × for lytic polypeptides.

The globular proteins β-galactosidase (Yamamoto et al., 1990) and the 140-kDa subunit of the sucrase isomaltase complex (Hunziker et al., 1986; residues 1008–1827) were also investigated. These proteins were used in vinculin hydrophobic labeling experiments as control, showing no labeling effect (Niggli et al., 1986). This result implies that the amino acid sequence of both proteins should neither enclose highly hydrophobic nor highly amphipathic regions. To check this assumption, the following test was applied to each of the proteins. With 21-residue windows within the amino acid sequence, the six most hydrophobic regions were selected. In addition, six regions with remarkably high hydrophobic moment values were selected. Of these hydrophobic and amphipathic regions, the 11-residue segment with the highest value for $\langle H\rangle$ or $\langle\mu_H\rangle$, was chosen. These data were then plotted in the Eisenberg diagram (Fig. 1) in which the open symbols indicate the results of β-galactosidase and the closed symbols the results of the sucrase isomaltase unit. As shown in Fig. 1, no amino acid protein segments for a lipid interaction via a monomeric transmembrane anchor or a surface-seeking helix could be observed.

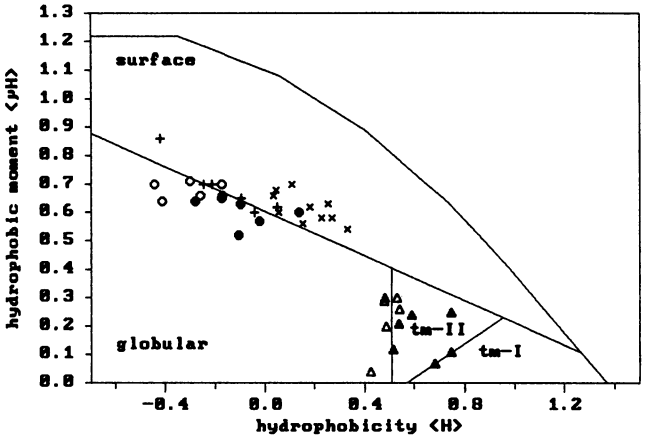

FIGURE 1 Eisenberg plot. Each point shows an 11-residue α-helix, with the ordinate representing the mean hydrophobic moment $\langle\mu_H\rangle$ and the abscissa representing the mean hydrophobicity $\langle H\rangle$. The equations for the straight lines, which separate different patterns of globular, surface, and transmembrane segments, are given in the Materials and Methods. The boundary curve defines the outer limit of possible points. (+) for polypeptide hormones or (×) for lytic polypeptides represent the most amphipathic 11-residue segments of these lipid-binding proteins. Data points (○, △) and (●, ▲) mark segments for β-galactosidase and for the 140-kDa subunit of the sucrase isomaltase complex, respectively. Circle or triangle symbols denote for both proteins each time six separate segments of maximal amphipathicity or hydrophobicity, respectively. *Surface,* surface-seeking region; *tm-I,* monomeric transmembrane region; *tm-II,* multimeric transmembrane region. (Analyzed polypeptide hormones are calcitonin, corticotropin-releasing factor, glucagon, vasoactive intestinal peptide, pancreatic polypeptide, calcitonin gene-related peptide. Analyzed lytic polypeptides are mangainin 1, bombolitin I, II, III, and V, crabrolin, mastoparan M, X, and C, and mastoparan Polistes.)

To check the validity of our prediction methods regarding lipid binding sites, we also carried out calculations (data not shown) for the sequence of pig cofilin (166 residues) (Matsuzaki et al., 1988). Cofilin is an actin-binding protein that interacts with acidic phosphoinositides. The exact lipid-binding region in the primary amino acid sequence of cofilin is known. Our calculations clearly predict a highly hydrophobic stretch in the primary amino acid region around residues 100–111. This stretch follows along the residues 112–118, a segment of positive charge. The secondary structure prediction for the residues 100–118 was identified as β-strand, interrupted by residues of high turn probability. The experimentally verified lipid-binding region of cofilin extends over the primary sequence residues 104–115 (Yonezawa et al., 1991).

Analysis of the 47-kDa talin fragment and the 32-kDa vinculin fragment

As described in the Introduction, the high affinity lipid-binding site(s) of talin and vinculin are localized in the small cleavage fragments of these proteins. Niggli and coworkers (1994) demonstrated by hydrophobic photolabeling as well as in co-sedimentation measurements with PS-liposomes that the NH_2-terminal 47-kDa fragment and not the COOH-terminal ~200-kDa fragment of human platelet talin specifically interacts with acidic liposomes. Johnson and Craig (1992, 1994) showed that the lipid-binding site(s) of chicken vinculin with acidic phospholipids are experimentally assigned to the 32-kDa fragment and not to the NH_2-terminal 90-kDa fragment. Computer analyses of the 47-kDa talin fragment and the 32-kDa vinculin fragment were carried out with the primary amino acid sequences of mouse talin, residues 1–433 (Rees et al., 1990) and of chicken embryo vinculin, residues 858–1066 (Coutu and

Craig, 1988). For comparison, the sequences of a talin homologue from *Dictyostelium* (Kreitmeyer et al., 1995) and of a vinculin homologue from nematode dense bodies (Barstead and Waterston, 1989) were also searched for lipid-binding sites.

Examining the 47-kDa talin sequence and the 32-kDa vinculin sequence for transmembrane stretches revealed that these proteins do not contain 21-residue-long stretches with a mean hydrophobicity greater than the minimal required value of 0.42 (Eisenberg et al., 1984). Domains of high hydrophobicity appear first at segment lengths ≤ 9. This behavior was examined and confirmed by two other amino acid hydrophobicity scales (Engelman et al., 1986; Jacobs and White, 1989). The hydrophobic interaction of vinculin with acidic lipids probably results from the incorporation of short hydrophobic stretches and/or attachment of amphipathic helical stretches. The secondary structure motif amphipathic α-helix appears to bind favorably to charged lipids, as polar and nonpolar faces of such helices facilitate electrostatic and hydrophobic forces to lipids. When the helical axis is aligned parallel to the membrane surface, the polar side of the amphipathic helix binds electrostatically to the charged lipid headgroups whereas the nonpolar helix side interacts in a hydrophobic way with the lipid chains.

An interesting feature of talin and vinculin are the different isoelectric points (pI) of the fragments compared with the intact molecules. Using the program ISOELECTRIC (GCG package), we ascertained for the 47-kDa mouse talin domain (residues 1–433) a pI of 8.4 and for the 200-kDa domain (residues 434–2541) a pI of 5.5 compared with a pI of 6.1 for the complete mouse talin molecule. Calculations by Coutu and Craig (1988) showed for the 32-kDa chicken vinculin fragment (residues 858–1066) a pI of 9.7 and for the 90-kDa fragment (residues 1–857) a pI of 5.4 compared with a pI of 5.9 for the whole protein. The pronounced basic character of the lipid-binding COOH-terminal domain of talin and the lipid-binding NH_2-terminal domain of vinculin indicates the importance of electrostatic forces between these fragments and acidic phospholipids.

Predictions for the 47-kDa talin fragment

Secondary structure predictions of the mouse talin region 1–433 result in a 49.2% content of α-helical structures separated by turn/coil regions of 37.2% and/or β-strands of 13.6% (Figs. 2*e* and 3*e*). The predictive algorithms, which determine the secondary structure of globular proteins in water, allocate to some short amino acid regions β-strand conformation. However, the conformation of a peptide domain for hydrophobic insertions into lipid membranes is widely assumed as α-helical (Jennings, 1989). Recent circular dichroism studies of synthesized, uncharged peptides in aqueous and micellar/vesicular media showed that the conformational preference of uncharged amino acids alters

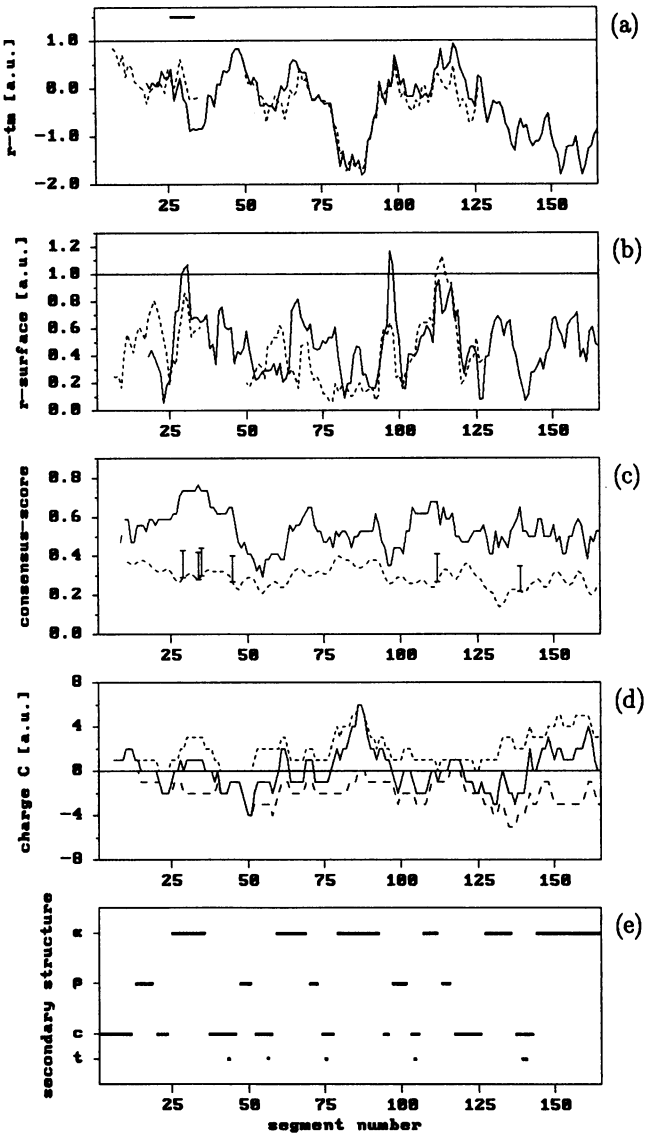

FIGURE 2 Structure prediction plots for the NH_2-terminal region of mouse talin (residues 1–165). Results for a talin homologue from *Dictyostelium* (residues 1–128) are plotted in (*a*) and (*b*) by dotted lines. The gaps in the lines of *Dictyostelium* talin are a result of the alignment of the *Dictyostelium* primary amino acid sequence to the mouse primary amino acid sequence. The horizontal bar in (*a*), (valid for (*a*)-(*e*)) indicates the proposed lipid-binding amino acid segment. (*a*) and (*b*) Plot of the ratios r_{tm} and $r_{surface}$ to evaluate hydrophobic stretches or amphipathic α-helical stretches for lipid binding (see Materials and Methods). Ratios $r \geq 1$ indicate amino acid stretches of high lipid-binding probability. The amino acid hydrophobicity scale of Eisenberg et al. (1984) was used and the amino acid window size was 11. (*c*) Matrix calculations for an amphipathic α-helix motif (see Appendix). At a window size of 18 residues, for every segment the consensus score of the existing sequence (continuous line) and the average consensus score of 400 sequence randomizations (dotted line) are plotted. For any segment the SD of the randomizations is denoted by a vertical bar if the SD factor Γ was >3.0. (*d*) Quantitative distribution of charged amino acids within 7-residue segments. The continuous, dotted, and discontinuous lines mark the sum of positively and negatively charged residues, only positively charged residues, and only negatively charged residues, respectively. (*e*) Prediction of secondary structure types α-helix (α), β-strand (β), random-coil (c) and turn (t) according to four different secondary structure algorithms as described in Materials and Methods. In (*a*)-(*d*) the results were plotted above the middle residue of the window.

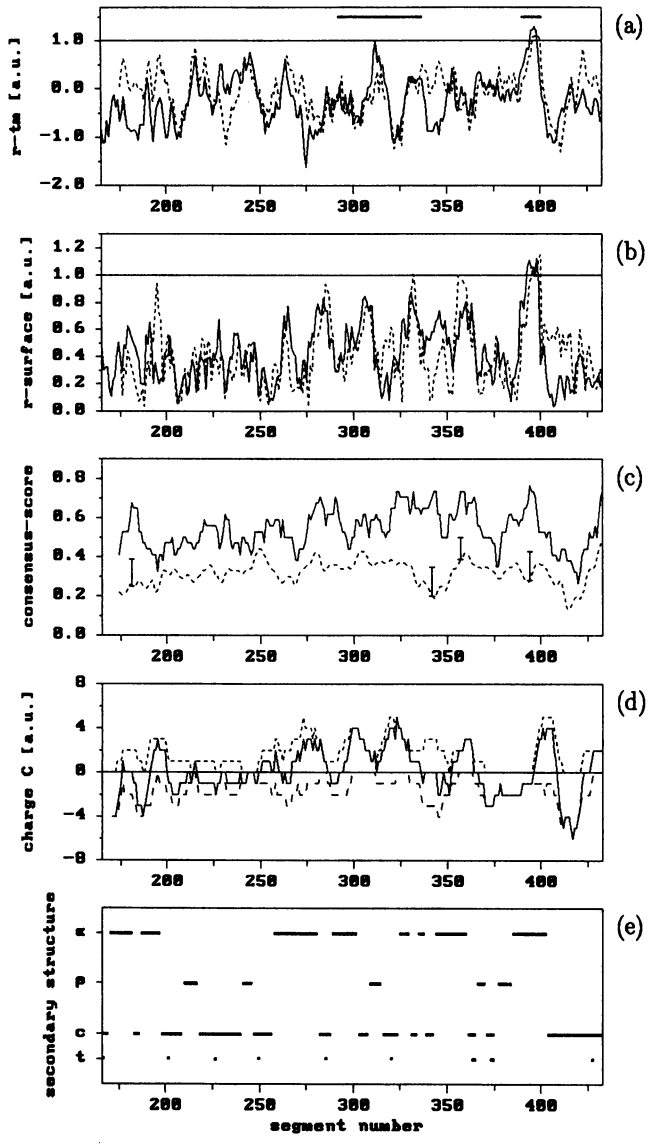

FIGURE 3 Structure prediction plots for the NH_2-terminal region of mouse talin (residues 166–433). The results for the talin homologue of *Dictyostelium* (residues 129–389) are plotted in (*a*) and (*b*) by dotted lines. The gap in the lines of *Dictyostelium* talin is a result of the alignment of the *Dictyostelium* primary amino acid sequence to the mouse primary amino acid sequence. The horizontal bars in (*a*), valid for (*a*)-(*e*), indicate the proposed lipid-binding amino acid segments. For detailed description of (a)-(e), see Fig. 2.

in response to the change in environment from water to lipid membranes (Li and Deber, 1994). Surprisingly, β-sheet-promoting amino acids in globular proteins (e.g., amino acid single letter code I, V, and T) turn out to be favorable helix promoters in lipid environments. As further demonstrated by Li and Deber (1994), the helical propensity of uncharged amino acids in membranes correlates with the hydrophobicity of amino acids. The importance of these findings can be demonstrated, e.g., at mouse talin sequence residues T-Y-G-V-S-F-F-L-V (position 307–315). The predictive methods classify this stretch as β-strand because the residues V and T, Y, F, and L show in aqueous media strong and moderate β-sheet-promoting properties, respectively (Chou and Fasman, 1978). However, the pronounced hydrophobic character, especially of the residues V, F, and L (Eisenberg et al., 1984), which is demonstrated around the segment number 310 (Fig. 3*a*, continuous line), attributes to the amino acid stretch a high tendency for α-helical structure in membranes.

The NH_2-terminal domain of mouse talin contains a segment (residues 165–373) that exhibits 20% identity with the NH_2-terminal domain of erythrocytes protein 4.1 (residues 1–208) (Rees et al., 1990). As shown by Cohen et al. (1988), the high affinity of protein 4.1 to acidic PS liposomes is mediated by the basic 30-kDa fragment that is derived from the NH_2-terminal end of protein 4.1 (residues 1–278). The homologous segment in mouse talin overlaps mostly with the acidic lipid-binding domain of protein 4.1. Therefore, the amino acid stretch 165–373 of the 47-kDa talin fragment was first examined for possible lipid-binding regions. The protein 4.1 (residues 1–278) was also searched for such regions.

Results from this analysis of mouse talin are shown in Fig. 3. The segment region 292–337 (primary amino acid sequence 287–342) may be relevant for the binding to negatively charged lipids. This region includes a short hydrophobic stretch surrounded by amphipathic, α-helical structures of remarkable positive charge. The hydrophobic stretch extends over the primary residues 305–315 and is shown at segment number 310 (Fig. 3*a*, continuous line). Although the secondary structure of the stretch 305–315 is predicted β-strand (Fig. 3*e*) in a lipid environment, the peptide structure is probably α-helical (see above). Both flanks of the hydrophobic stretch have a moderate surface-seeking propensity (see Fig. 3*b*, continuous line) around segment 303 and segment 328, and the arrangements of the residues agree well with the amphipathic helix motif (Fig. 3*c*). The secondary structure of the amphipathic regions, which extend over the primary amino acid residues 287–305 and 325–342, is predicted α-helical (Fig. 3*e*). Within the residue region 316–324, which is predicted as random/coil, a turn is probably around residue 320 (see Fig. 3*e*). The fraction of positive amino acids in the amphipathic α-helices is very high (residues 287–305 and 325–342; see Fig. 3*d*). This feature is also reflected by the calculated pI = 10.8 for the amino acid region 287–342.

In contrast to predictions for the talin residues 165–373, the homologous region of protein 4.1 (residues 1–208) indicates more clearly amphipathic and especially hydrophobic stretches (data not shown). It is intriguing that by far the most hydrophobic stretch of the 30-kDa fragment of protein 4.1, residues 1–278, is located between residues 208 and 278 (data not shown). This finding shows that the lipid-binding site(s) of the talin 47-kDa fragment must not be inevitably in the amino acid region 165–373; probably there are other strong binding sites in the regions 1–165 and 374–433.

Computational results of the primary amino acids 1–165 of mouse talin are summarized in Fig. 2. No region of

significant hydrophobic character can be detected within the examined amino acid range (Fig. 2*a*, continuous line). However, around segment positions 29 and 95, amino acid configurations are predicted of obvious surface-seeking character (Fig. 2*b*, continuous line), suggesting lipid interactions via an amphipathic helix. The primary amino acid limits of the first of these amphipathic regions are selected according to the predicted α-helix range 21–39 (Fig. 2*e*); within this amino acid range for 9 of the 19 residues, three or all of the secondary structure prediction methods classify the structure as α-helical. The average charge of the stretch is positive (Fig. 2*d*). The amino acid composition and arrangement of residues 21–39 is most notable with regards to the amphipathic helix motif (Fig. 2*c*); no amino acid stretch in the entire 47-kDa talin sequence reaches higher consensus score values. The probability that the given amphipathic arrangement of residues occurs by chance is very small (Fig. 2*c*, vertical bars). Therefore, the strong amphipathic structure of residues 21–39 seemed good candidates for membrane interactions.

The other amphipathic stretch around segment number 95 (Fig. 2*b*, continuous line) appears to have unfavorable preconditions for lipid binding. (1) The amphipathic stretch, which is limited by a proline at position 87 and a turn around residue 104, has a secondary structure prediction of random/coil and β-strand (Fig. 2*e*). (2) The molecular agreement of the residues 88–103 with the amphipathic helix motif and the statistical significance of the amphipathic order of these residues are small (Fig. 2*c*). (3) The amino acid stretch 88–104 has a negative mean charge (Fig. 2*d*). Although the highly, positively charged region before the amphipathic helix (primary amino acid sequence 73–87; Fig. 2*d*) could serve as a promoter for lipid interactions, the lipid-binding propensity of the region 88–104 is classified as weak.

The most probable region in the NH_2-terminal mouse talin fragment for lipid interactions of significant hydrophobic character was discovered in the amino acid range 373–433 (Fig. 3). Within this range around segment number 394, calculations predict a surface-seeking region (Fig. 3*b*, continuous line) which is markedly hydrophobic in nature (Fig. 3*a*, continuous line). The secondary structure type of the primary amino acid residues 385–401 is α-helical (Fig. 3*e*), as only 1 of these 19 residues is not predicted by three or all secondary structure prediction methods as α-helical. The primary amino acid residues 385–401 generate an approximate five-loop α-helix with two strikingly different surface sides. One-third of the helix surface is composed of only charged and polar residues whereas the other two-thirds of the helix surface have a very hydrophobic character caused by five extremely hydrophobic isoleucin residues (Eisenberg et al., 1984). These residues show only a mean consensus with the amphipathic helix motif because of the quantitative assymmetrical distribution of polar and nonpolar residues on the helical sides (Fig. 3*c*). The amphipathic arrangement of these residues is statistically significant in comparison with random arrangements (see Fig. 3*c*, vertical bar). An interaction of the residues 385–401 with acidic lipids could be induced by the very positive amino acid stretch K-K-K-S-K located at sequence 402–406. The positively charged part can be recognized in Fig. 3*d* around segment numbers 401–405. Therefore, primary amino acid range 385–406 is a good candidate for lipid binding.

Analyses carried out for a talin homologue from *Dictyostelium* (2490 residues; Kreitmeyer et al., 1995) compared well with mouse talin. The alignment of the two complete protein sequences shows a similarity of 46% and an identity of 24%. The fit is best between the NH_2-terminal regions where the *Dictyostelium* talin residues 1–389 and the mouse talin residues 1–428 are 66% similar and 44% identical. In *Dictyostelium* talin, stretches of 4 residues and 37 residues are missing that correspond to the primary amino acid regions 40–43 and 131–167 of mouse talin. Taking into account these two gaps, the calculated ratios r_{tm} and $r_{surface}$ for *Dictyostelium* talin residues 1–389 are plotted in Figs. 2,*a* and *b*, and 3, *a* and *b* (dotted lines). Within the mouse talin primary amino acid sequence 1–433, three regions for lipid-binding are proposed, two amphipathic α-helices along the residue stretches 21–39 and 385–406 and a mixture of hydrophobic/amphipathic α-helices along the residue stretch 287–342. By comparing the ratios r_{tm} and $r_{surface}$ of the mouse talin sequence with the aligned sequence of *Dictyostelium* talin, it is observed that 1) *Dictyostelium* talin shows around the segment numbers 26–34 no marked surface-seeking propensity (Fig. 2*b*, dotted line) and around the segment number 310 only a weak hydrophobic character (Fig. 3*a*, dotted line), 2) and around segment number 397 the primary sequence residues 348–364 of *Dictyostelium* talin form a surface-seeking domain (Fig. 3*b*, dotted line) of pronounced hydrophobic character (Fig. 3*a*, dotted line), which is in good agreement with mouse talin. These observations suggest that the residues around segment position 397 include the prominent lipid-binding site of mouse talin and present a possible general domain for various talin species. Two specific lipid-binding sites for mouse talin are assumed for primary sequence region 21–39 and 287–342.

Predictions for the 32-kDa vinculin fragment

Secondary structure prediction analysis of the chicken embryo vinculin fragment (residues 857–1066) indicates a 61.7% content of α-helical structures separated by some turn/coil regions of 35.9% and/or short β-strands of 2.4%. The proline-rich region 860–878 is predicted to be of turn/coil structure (Fig. 4*e*).

Within the sequence of the 32-kDa chicken vinculin fragment, no 11-residue fragments are found that are sufficient for pure hydrophobic anchoring to lipid bilayers (Fig. 4*a*, continuous line). This finding suggests that the hydrophobic binding of the 32-kDa vinculin fragment to acidic phospholipids is effected by amphipathic structures. How-

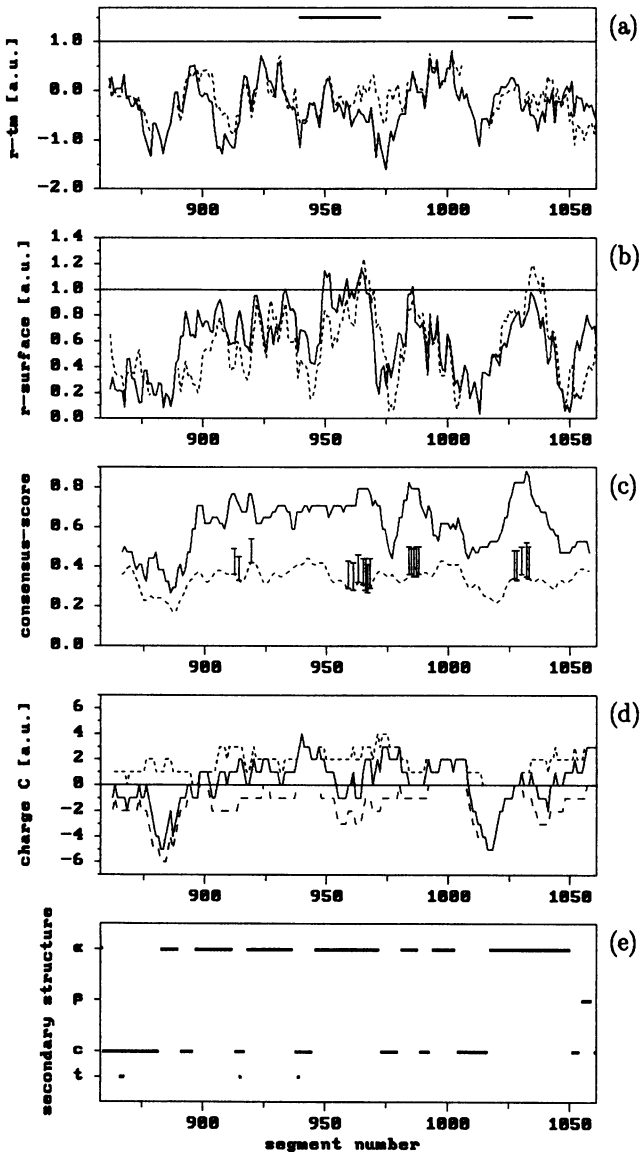

FIGURE 4 Structure prediction plots for the COOH-terminal region of chicken embryo vinculin (residues 858–1066). Results for the vinculin homologue of nematode dense bodies (residue regions 786–812, 819–945, and 955–1009) are plotted in (*a*) and (*b*) by dotted lines. The positions of the three nematode vinculin sequence fragments to chicken vinculin present the best alignment of both protein primary amino acid sequences. The horizontal bars in (*a*), valid for (*a*)-(*e*), indicate the proposed lipid-binding amino acid segments. For detailed description of (*a*)-(*e*), see Fig. 2.

ever, around segment numbers 950–969 (primary amino acid sequence 945–974), a surface-seeking region of distinct amphipathic structure is identified (Fig. 4*b*, continuous line). The secondary structure prediction for this 30-residue-long segment is α-helical (Fig. 4*e*); for 22 of the residues, three or all of the used secondary structure methods suggest an α-helical structure. Examination of the amino acids 945–974 revealed that the surface of the approximately eight-loop α-helix can be divided into a polar and a nonpolar side of ~40% and ~60%, respectively. The polar side is composed entirely of positive, negative, and polar amino acids whereas the nonpolar side consists mainly of hydrophobic and neutral amino acids. The pronounced polar/nonpolar structure is confirmed by results of helix motif calculations in Fig. 4*c*. The high consensus score values of the segments 959–967 reflect the obvious amphipathic character. Furthermore, randomizations of the residues in the range 945–974 indicate that the existing amphipathic grouping of these residues are of high statistical significance (see Fig. 4*c*, vertical bars); e.g., the probability that the 18-residue segment 967 will form an amphipathic structure at random is 10^{-4}, based on a normal distribution.

Analyses of the distribution of charged amino acids in the close vicinity of the residues 945–974 show that before and after this region short stretches of positive average charge are located. With regard to the primary amino acid sequence, the extension of these stretches is restricted to residues 935–944 and 975–978 (Fig. 4*d*). Each of these segments include three positively and no negatively charged amino acids. The secondary structure prediction for both segments is random/coil (Fig. 4*e*). As these two positive segments may play an important role for an initial attachment of vinculin to acidic phospholipids, the total length of the lipid-binding domain is fixed to residues 935–978. It is important to mention that the calculated pI of these 44 residues is 11.0.

Another region in the 32-kDa vinculin domain, which could bind in an amphipathic way two acidic phospholipids, is the amino acid region 1020–1040. As shown in Fig. 4*b* (continuous line), the segments around 1035 have a mean surface-seeking propensity although the composition and the order of the 18-residue segments 1029–1031 agree well with the amphipathic helix motif (Fig. 4*c*). The predicted secondary structure for residues 1020–1040 is α-helical (Fig. 4*e*), as for 19 of the 20 residues three or all of the secondary structure prediction methods indicate an α-helical structure. The average charge of this region is more or less positive (Fig. 4*d*). It is interesting to note that the program PEPCOIL (GCG package), which is used for the determination of α-helical coiled-coil structures in proteins, predicts with 65% probability a coiled-coil region in the vinculin amino acid range 1014–1045.

Analyses were also carried out for vinculin of nematode dense bodies (1010 residues; Barstead and Waterston, 1989), which show a high degree of homology with chicken embryo vinculin. The alignment of the primary sequences by BESTFIT (GCG package) showed that these two proteins are ~65% similar and ~47% identical. The nematode vinculin tail 786–1010 was aligned to chicken vinculin tail 858–1066 with 79% similarity and 62% identity. BESTFIT analysis showed that within the chicken vinculin tail (residues 858–1066) one stretch of 5 residues and another stretch of 9 residues were missing, corresponding to the primary amino acid sequence regions 813–818 and 946–954 of nematode vinculin. To plot chicken vinculin without gaps against the nematode vinculin, the gap stretches were neglected in nematode vinculin calculations and only sequence regions 786–812, 819–945, and 955–1010 were

examined. The calculated ratios r_{tm} and $r_{surface}$ for these nematode vinculin regions are given in Fig. 4,*a* and *b* (dotted lines). Within the chicken vinculin primary amino acid region 858–1066 the residue stretches 935–978 and 1020–1040 are believed to bind via amphipathic α-helices to the surface of lipid bilayers. The following results were obtained by comparing the ratios r_{tm} and $r_{surface}$ of the chicken vinculin sequence with the aligned sequence of nematode vinculin: near segment numbers 964–968 and 1028–1035, the primary amino acid sequence residues of nematode vinculin 893–907 and 966–983 form domains with pronounced surface-seeking character (Fig. 4*b*, dotted line). This conveys that the two suggested lipid-binding regions of chicken embryo vinculin (residues 935–978 and 1020–1040) are confirmed by analyses of the nematode vinculin tail sequence. These two amino acid regions could present general domains of various vinculin species.

DISCUSSION

The anchorage of actin-associated proteins to the plasma membrane has been of interest for many years as it is believed that these proteins probably stabilize the cytoskeleton within cells (cf. the review of Isenberg, 1991; Isenberg and Goldmann, 1992, 1995).

Here, we have examined the cytoskeletal proteins talin and vinculin by computer analysis on possible lipid-binding site(s) as Niggli et al. (1994) and Johnson and Craig (1992, 1994) demonstrated in various experiments that the NH_2-terminal 47-kDa talin fragment and the COOH-terminal 32-kDa vinculin fragment, respectively, carry the high affinity binding site(s) with phospholipids. The interaction of both proteins with lipids appears to include hydrophobic and electrostatic forces as hydrophobic labeling experiments indicate (partial) insertion into the lipid bilayer and as the protein binding depends on the presence of acidic phospholipids. Suggestions for interactions of proteins with acidic or anionic lipids were described by DeKruijff (1994). Negatively charged lipids, by virtue of their charge, localize the protein by electrostatically interacting with positively charged domains on proteins. The initial electrostatic interaction then facilitates subsequent insertion of (or part of) the protein into the membrane, which could involve, e.g., hydrophobic stretches of the protein.

In thermodynamic terms, the insertion of a polypeptide into a membrane is energetically most favorable if an ordered secondary structure like α-helix or β-barrel exists already in aqueous solution (Engelman et al., 1986). An examination of secondary structure predictions for the 47-kDa (mouse) talin fragment and the 32-kDa (chicken embryo) vinculin fragment clearly showed that none of the fragments included a region with the ability to form β-barrels. The structure predictions were confirmed by circular dichroism analysis of the talin molecule, which revealed no significant β-barrel content (Molony et al., 1987). Furthermore, the structure of the vinculin tail was proposed to be a linearly extended α-helix (Coutu and Craig, 1988). Therefore, our search for lipid-binding regions concentrated on hydrophobic or amphipathic α-helices.

The computer analysis of the primary amino acid sequences of the 47-kDa talin fragment and the 32-kDa vinculin fragment based on four methods. (1) To detect within protein sequences hydrophobic or amphipathic regions of high lipid-binding probability, we used the well known Eisenberg plot (Eisenberg et al., 1984). We used a window size of 11 for two reasons. First, calculations with the window dimension of 21 showed that neither the 47-kDa talin fragment nor the 32-kDa vinculin fragment contained transmembrane amino acid segments. Therefore, the window size was decreased to 11 to be sensitive for all possible lipid-binding segments. Second, the results of the Eisenberg plot belong to 11-residue-long fragments. (2) To gain insight into the arrangement of physicochemically different amino acids along α-helices of remarkable amphipathic character, we introduced a new matrix motif method. (3) The location of positively and negatively charged amino acids within the examined protein sequences might play an important role for lipid interactions; therefore, charge distributions were calculated. (4) Secondary structure predictions were determined to find, e.g., residues of high turn probability.

The examination of the 47-kDa fragment of mouse talin (residues 1–433) exhibited the following features. (1) The NH_2-terminal talin fragment is basic in nature (pI = 8.4), and the dominant secondary structure type is 49% α-helical. (2) No transmembrane segment(s) of 18–21 residues can be detected. Highly hydrophobic regions are determined for segment sizes $\leq$9. (3) Residues 21–39 form an α-helix of pronounced amphipathic character and positive mean charge. (4) Within the amino acid region 165–373, which is homologous partly with the lipid-binding domain of protein 4.1 (Rees et al., 1990), along residues 287–342 a short hydrophobic stretch surrounded by positively charged amphipathic α-helices is observed. (5) Residues 385–401 build an amphipathic α-helix of extensive hydrophobic surface side. This α-helix is followed by a short, extremely positive amino acid stretch (residues 402–406). (6) Comparing analyses of the mouse talin sequence with the aligned sequence of the talin homologue from *Dictyostelium* confirm the surface-seeking stretch 385–401 in mouse talin. The *Dictyostelium* talin regions, which correspond to the mouse talin primary amino acid sequence regions 21–39 and 287–342, show low lipid-binding probability.

The analysis of the 32-kDa fragment of chicken embryo vinculin (residues 858–1066) showed the following features. (1) The COOH-terminal vinculin fragment is very basic in nature (pI = 9.7) and has a 62% content of the secondary structure type α-helix. (2) No transmembrane segment(s) of 18–21 residues can be detected. Highly hydrophobic regions are determined for segment sizes $\leq$9. (3) Along the primary amino acid sequence 945–974 an approximately eight-loop α-helix with distinct amphipathic structure was observed. On both sides of this helix, short

random-coil stretches of positive mean charge are localized (residues 935–944 and 975–978). (4) The region 1020–1040 forms an α-helix of remarkable amphipathic character and of weak positive mean charge. (5) Comparing the chicken embryo sequence with the aligned sequence of a vinculin homologue of nematode dense bodies confirmed both surface-seeking stretches 945–974 and 1020–1040 in chicken embryo vinculin.

Within the COOH-terminal region of chicken vinculin, both the paxillin-binding site and the focal contact targeting sequence were mapped to a region confined by residues 979–1028 (Wood et al., 1994). The paxillin/focal contact binding domain does not overlap with the suggested lipid-binding domain 935–978 but partly with the lipid-binding domain 1020–1040. The F-actin-binding domain on the vinculin tail, localized within the residue region 893–1016 (Menkel et al., 1994), shows a complete overlap with the proposed lipid-binding domain 935–978, but no overlap with domain 1020–1040. The importance of residue regions 935–978 and 1020–1040 as possible lipid-binding sites could be directly examined in lipid-binding studies in the absence or presence of F-actin and paxillin, respectively.

The determined lipid-binding regions of talin and vinculin suggest protein attachment to lipid bilayers via amphipathic α-helices parallel to the membrane surface. Such protein-membrane coupling is not restricted to small peptides, e.g., polypeptide hormones or lytic polypeptides (17–26 residues), as recently shown for the globular enzyme prostaglandin H_2 synthase (577 residues; Merlie et al., 1988); based on x-ray crystallography, the membrane-binding domain of this enzyme is a motif of three short amphipathic helices positioned in a parallel way to the plane of the membrane (Picot and Garavito, 1994). We believe that talin and vinculin incorporate only in one leaflet of lipid bilayers. According to Blobel's classification of membrane proteins (Blobel, 1980), talin and vinculin would therefore be regarded as monotopic membrane proteins.

Here, we illustrate the physical size of the predicted amphipatic α-helices, using vinculin residues 945–974. Assuming for a helix the geometry of a tube, the 29 residues of the (chicken embryo) vinculin sequence form a tube of ~43 Å length and approx 12 Å in mean diameter (A. Lupas, personal communication), and viewing this tube perpendicular to its axis, the projected area is 516 $Å^2$ and the perimeter of this area is 110 Å. We estimate the square area per lipid in membranes as 65 $Å^2$. Provided the amphipathic helix of vinculin is incorporated into the membrane in parallel orientation, this helix occupies an area equivalent to ~8 lipid molecules that is surrounded by ~13–14 lipid molecules.

CONCLUSIONS

We have shown by computer analysis that talin and vinculin of different species interact with acidic phospholipids. The available computer data suggest specific interaction of residues 21–39, 287–342, and 385–406 of the 47-kDa mouse talin fragment with acidic phospholipids. Mouse talin (primary amino acid sequence 385–401) and *Dictyostelium* talin (primary amino acid sequence 348–364) could possibly express a general lipid-binding domain for talin of different species. So far no experimental evidence has been published confirming our assumptions.

However, for vinculin the calculated primary sequence residue region 935–978 has basically been confirmed as a good candidate for a lipid-binding site. Johnson and Craig (1992) showed on their poster (American Society of Cell Biologists Meeting, 1992) that the region 916–970 binds to acidic phospholipids (personal communication; this information was not included in their abstract). The calculations of a possible second binding site on the 32-kDa chicken embryo vinculin fragment (primary amino acid sequence 1020–1040) still awaits confirmation. As these two amino acid regions are conserved with high homology in the sequence of nematode vinculin, both regions could constitute general lipid-binding domains of different vinculin species.

The close association of vinculin and talin with membrane phospholipids and the proposed interaction of these proteins is likely to be important for cell adhesion and focal contact assembly (Samuels et al., 1993). Proposed experiments with high priority are to examine the effect of the deletion of these important domains at the NH_2 terminus of talin and the COOH terminus of vinculin.

APPENDIX

Matrix motif method for the determination of amphipathic α-helices

The basic idea of this method was taken from the work of Hazelrig et al. (1993). The main features of the model are explained below.

If amino acids along the axis of a helix are projected onto a plane, the consecutive residues of an ideal α-helix (periodicity 3.6) are spaced at 100° intervals. The model assumes an ideal α-helix of five loops or a segment length of 18. Supposing a segment of 18 residues, there is one residue for every 20° interval. Fig. A1 shows the projected residue distribution of a five-loop α-helix. The numbers outside of the circle mark the order of the projected residues in clockwise direction. The numbers inside the circle give the order of the residues in the primary sequence if the position of the first primary sequence residue agrees with the position of the first projected residue. The terms *hydrophobic/membrane side* and *polar/solvent side* in Fig. A1 indicate typical properties of an amphipathic helix and the orientation of such a helix interacting with lipid membranes.

In the matrix method, amino acids are classified into five physicochemical groups: hydrophobic (amino acid single letter code F, M, I, L, V, W, and C), polar (Q and N), positive (K, R, and H), negative (E and D), and neutral (Y, P, S, G, T, and A) (Segrest et al., 1992). Regarding the distribution of these amino acid groups in amphipathic helices, it is assumed that these helices can be divided into three spatial sectors (see Fig. A1): (1) a hydrophobic sector I that interacts with the hydrophobic core of the lipid membrane, (2) an interface sector II that is defined by the lipid headgroups, and (3) a polar sector III that is believed to interact with the solvent; i.e., sector I (outside numbers 1, 2, 3, 17, and 18) should comprise hydrophobic amino acids, in sector II (outside

numbers 4–7 and 13–16) positive and polar amino acids should be present, and sector III (outside numbers 8–12) should include charged and polar amino acids. Neutral amino acids can be located at every helix position. This proposed assignment of amino acid groups was deduced from the properties found in the lipid-binding, amphipathic helices of apolipoproteins, polypeptide hormones, and lytic polypeptides (cf. Segrest et al., 1990).

The exact composition of the amphipathic helix motif was mathematically defined by a matrix, hereafter referred to as motif matrix M_{ij}. This matrix always has five rows (i = 1–5), which are assigned to the five amino acid groups; i = 1 for hydrophobic, i = 2 for polar, i = 3 for positive, i = 4 for negative, and i = 5 for neutral residues. If there is an 18-residue amphipathic helix, the motif matrix is composed of 18 columns (j = 1–18) with each column being assigned to one of the residues shown in Fig. A1, outside numbers. The components M_{ij} of the motif matrix are integer numbers between −2 and 2. These numbers are supposed to weight the various amino acid groups at every position of the amphipathic helix motif. The values for the weighting are determined according to a simple rule. The more (or the less) the amino acid group at a certain helix position fulfills the constraints of the amphipathic motif, the more positive (or negative) the value of the weighting is. Considering the sectors I, II, and III described above, the weighting of the amphipathic helix motif matrix is:

$$M_{ij} = \begin{pmatrix} 2 & 2 & 2 & 1 & 1 & 1 & 0 & -1 & -2 & -2 & -2 & -1 & 0 & 1 & 1 & 1 & 2 & 2 \\ -2 & -1 & 0 & 1 & 1 & 2 & 2 & 2 & 2 & 2 & 2 & 2 & 2 & 2 & 1 & 1 & 0 & -1 \\ -2 & -1 & 0 & 1 & 1 & 2 & 2 & 2 & 2 & 2 & 2 & 2 & 2 & 2 & 1 & 1 & 0 & -1 \\ -2 & -2 & -2 & -2 & -2 & -1 & 0 & 2 & 2 & 2 & 2 & 2 & 0 & -1 & -2 & -2 & -2 & -2 \\ 1 & 1 & 1 & 1 & 1 & 1 & 1 & 1 & 1 & 1 & 1 & 1 & 1 & 1 & 1 & 1 & 1 & 1 \end{pmatrix}$$

(Note that the defined values should be considered only as propositions.)

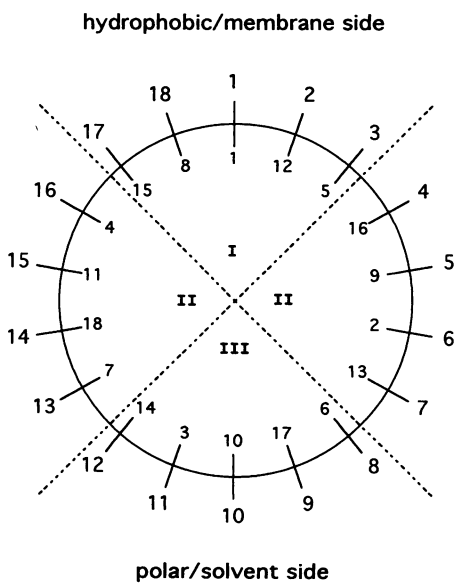

FIGURE A1 Assumed structure of an amphipathic, ideal α-helix of 18 residues (or five loops) by the matrix method. The distribution of residues along the helical axis is shown in a plane projection. Numbers outside of the circle mark the order of the projected residues in clockwise direction, whereas the numbers inside mark the order of the primary amino acid sequence residues. An amphipathic helix is supposed to consist of three spatial sectors, a hydrophobic, membrane-incorporated sector I, an interface region for lipid-headgroup interaction, sector II, and a polar, solvent-environed sector III.

To test the compatibility of a given amino acid segment with the amphipathic motif, an additional matrix is necessary, hereafter referred to as segment matrix S_{jk}. This matrix gives information about the assignment of each amino acid in the segment to defined amino acid groups. S_{jk} is always composed of five columns (k = 1–5) for the five amino acid groups; k = 1 for hydrophobic, k = 2 for polar, k = 3 for positive, k = 4 for negative, and k = 5 for neutral residues. Analogous to the motif matrix M_{ij} the index j for the rows of S_{jk} denotes the sequence of the helix residues and has the range j = 1–18. The components of S_{jk} can have the integer values 0 and 1. Here, the weighting is explained by an example. Supposing at position 10 of a segment is a positive amino acid, the matrix elements of row 10 have the values $S_{10\text{-}1} = 0$, $S_{10\text{-}2} = 0$, $S_{10\text{-}3} = 1$, $S_{10\text{-}4} = 0$, and $S_{10\text{-}5} = 0$.

For comparison of an 18-residue segment (matrix S_{jk}) with the amphipathic helix motif (matrix M_{ij}) a comparison matrix C_{ik} is calculated from the product of both matrices M_{ij} and S_{jk}:

$$C_{ik} = \sum_{j=1}^{18} M_{ij} S_{jk}$$

Then, by summation over all components of C_{ik} a consensus score is determined:

$$\text{consensus score} = \left(\sum_{i=1}^{5} \sum_{k=1}^{18} C_{ik} \right) / C_{max}.$$

The factor C_{max} is given by the maximum positive value possible for the consensus score:

$$C_{max} = \sum_{j=1}^{18} \max(M_{ij}),$$

where $\max(M_{ij})$ denotes the highest weighting value of matrix column j. Normalizing on C_{max}, the maximum possible value of the consensus score is ≤1. By definition, for any amino acid segment only the maximum possible consensus score is of interest. This maximum score results from the following procedure. The residues of a segment are rotated 18 times at 20° increments around the axis of the helical motif (see Fig. A1). After every rotation the consensus score is calculated and then by comparison the maximum score is determined.

With regard to the amino acid composition and arrangement, the value of the consensus score is considered as a quantitative measure for the compatibility between a given amino acid segment and the amphipathic motif. To improve the meaningfulness of this value, it is related to the mean value and SD of random permutations of the same amino acid segment. In this way it is known whether the amphipathic arrangement of the segment residues is statistically significant in comparison with arrangements at random. The following SD factor Γ is defined for the consensus score:

$$\Gamma(\text{consensus score}) = (\text{consensus score} - \langle \text{consensus score} \rangle_R)/\sigma_R$$

where $\langle \text{consensus score} \rangle_R$ and σ_R are the mean value and the SD of 400 random permutations of the segment amino acid sequence. The probability that the residues of a segment do not form an amphipathic structure by chance increases with rising values for Γ(consensus score).

To ascertain the matrix method efficiency, the computations for the highly amphipathic, lipid-binding apolipoprotein AI are plotted in Fig. A2*a*. According to the defined 18-residue-long helix motif, an 18-residue window was run along the entire protein sequence. The continuous and the discontinuous lines represent values for consensus score and $\langle \text{consensus score} \rangle_R$, respectively. The vertical bars display σ_R values of segments with Γ(consensus score) >3.3. The horizontal bars indicate the limits of domains that associate in an amphipathic way with phospholipids. These domains were shown in synthetic peptide experiments (cf. Segrest et al., 1992). The profile in Fig. A2*b* gives the result of the calculation of the average hydrophobic moment (periodicity 3.6) to evaluate amphipathic α-helices (Eisenberg et al., 1982).

It is observed in Fig. A2*a* that the marked amphipathic character of apolipoprotein AI is reflected by high average consensus score values. For each of the lipid-binding domains, segments can be found where the amphipathic formation of the segment residues is statistically significant (Fig. A2*a*, vertical bars). This implies that this matrix method detects adequately the amphipathic, lipid-binding regions within the sequence of the apolipoprotein. The amphipathic regions determined under experimental conditions are also confirmed by the hydrophobic moment analysis. It is interesting that this method, somewhat different to the matrix method, suggests a highly amphipathic stretch in the amino acid range 1–33. This stretch, however, shows no interaction with phospholipids (cf. Segrest et al., 1992).

Amino acid segments proposed for lipid binding

In Fig. A3 we show the short amino acid segments for talin and vinculin of different species that are identified by our prediction methods to bind to acidic phospholipids. The relevant lipid-binding amino acids are underlined in Fig. A3.

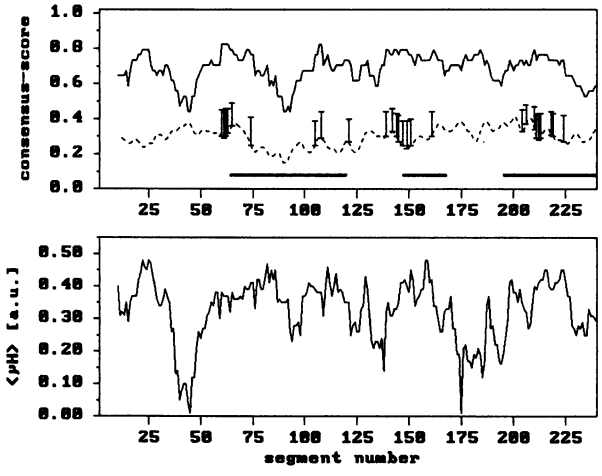

FIGURE A2 An example of the matrix method: apolipoprotein AI (249 residues), a highly amphipathic α-helical lipid-binding protein. The segment window size for (*a*) and (*b*) was 18, and the results were plotted above the middle residue of the window. (*a*) Matrix calculations for the amphipathic α-helix motif. The consensus score of the existing sequence (discontinuous line) and the average consensus score of 400 sequence randomizations (dotted line) are plotted for every 18-residue segment. The SD of the randomizations is marked by a vertical bar if the SD factor Γ was >3.3. Horizontal bars indicate primary amino acid sequence regions that are experimentally proved as lipid binding. (*b*) Mean hydrophobic moment $\langle \mu_H \rangle$ (periodicity 3.6) for the evaluation of amphipathic α-helices.

(a) Talin

```
15  KTMQFEPSTMVYDACRMIRERIPEALAGPPN  45   mouse (21-39)

285 NCGQMSEIEAKVRYYVKLARSLKTYGVSFFLV 315  mouse (287-342)
316 KEKMKGKNKLVPRLLGITKECVMRVDEKTKE  346

380 VQTTEGEQIAQLIAGYIDIILKKKKSKDHFG 410  mouse (385-406)
    :||.:.|||.|||:|||:||:| :|.... .
342 LQTPNPEQISQLIGGYIEIIMKARKDSSK.V 372  Dicty. (348-364)
```

(b) Vinculin

```
925 RMALLMAEMSRLVRGGSGNKRALIQCAKDIA 955  chicken (935-974)
    |||:||| :|.||||::|.|:.||.|.|.||
859 RMAILMARLSQLVRGEGGTKKDLINCSKAIA 889  nematode
956 KASDEVTRLAKEVAKQCTDKRIRTNLLQVCE 986  chicken
    ..|:|||||| ::|: ||| ::||.||||:|
890 DSSEEVTRLAVQLARLCTDIKMRTALLQVSE 920  nematode (893-907)

1015 ESEQATEMLVHNAQNLMQSVKETVREAEAAS 1045 chicken (1020-1040)
     |.::| : ||||||||||||||:.||.||||
958  EDDEAMQQLVHNAQNLMQSVKDVVRAAEAAS 988  nematode (966-983)
```

FIGURE A3 Segments of primary amino acid sequences proposed for lipid interaction. Underlined positions mark possible lipid-binding amino acids. (*a*) Sequences from mouse and *Dictyostelium* talin. (*b*) Sequences from chicken embryo and nematode vinculin. The numbers within parentheses indicate the limits of the lipid-binding segments. The alignment and the resulting similarities of the sequences with each other are partly shown. I, identities; :, conservative substitutions; ., low similarities.

This work was supported by the Deutsche Forschungsgemeinschaft (SFB 266) to G. I. and E. S., and by grants from NATO (CRG 940666 and DFG Go 598/3-1) and the American Cancer Society to W. H. G. We thank Dr. R. M. Ezzell for stimulating discussions and Ms. C. Meissner for careful reading of this manuscript.

REFERENCES

Barstead, R. J., and R. H. Waterston. 1989. The basal component of the nematode dense-body is vinculin. *J. Biol. Chem.* 264:10177–10185.

Beckerle, M. C., T. O'Halloran, and K. Burridge. 1986. Demonstration of a relationship between talin and P235, a major substrate of the calcium-dependent protease in platelets. *J. Cell. Biochem.* 30:259–270.

Beckerle, M. C., and R. K. Yeh. 1990. Talin: role at sites of cell-substratum adhesion. *Cell Motil. Cytoskeleton* 16:7–13.

Belkin, A. M., and V. E. Kotelianski. 1987. Interaction of iodinated vinculin, metavinculin and α-actinin with cytoskeletal proteins. *FEBS Lett.* 220:291–294.

Blobel, G. 1980. Intracellular protein topogenesis. *Proc. Natl. Acad. Sci. USA.* 77:1496–1500.

Burridge, K., and P. Mangeat. 1984. An interaction between vinculin and talin. *Nature.* 308:744–746.

Chou, P. Y., and G. D. Fasman. 1978. Empirical predictions of protein conformation. *Annu. Rev. Biochem.* 47:251–276.

Cohen, A. M., S. C. Liu, J. Lawler, L. Derick, and J. Palek. 1988. Identification of the protein 4.1 binding sites to phosphatidylserine vesicles. *Biochemistry.* 27:614–619.

Coutu, M. D., and S. W. Craig. 1988. cDNA-derived sequence of chicken embryo vinculin. *Proc. Natl. Acad. Sci. USA.* 85:8535–8539.

Crawford, A. W., J. W. Michelsen, and M. C. Beckerle. 1992. An interaction between zyxin and α-actinin. *J. Cell Biol.* 116:1381–1393.

DeKruijff, B. 1994. Anionic phospholipids and protein translocation. *FEBS Lett.* 346:78–82.

Devereux, J., P. Haeberli, and O. Smithies. 1984. A comprehensive set of sequence analysis programs for the VAX. *Nucl. Acids Res.* 12:387–395.

Dietrich, C., W. H. Goldmann, E. Sackmann, and G. Isenberg. 1993. Interaction of NBD-talin with lipid monolayers: a film balance study. *FEBS Lett.* 324:37–40.

Eimer, W., M. Niermann, M. A. Eppe, and B. M. Jockusch. 1993. Molecular shape of vinculin in aqueous solution. *J. Mol. Biol.* 229:146–152.

Eisenberg, D., E. Schwarz, M. Komaromy, and R. Wall. 1984. Analysis of membrane and surface protein sequences with the hydrophobic moment plot. *J. Mol. Biol.* 179:125–142.

Eisenberg, D., R. M. Weiss, and T. C. Terwillinger. 1982. The helical hydrophobic moment: a measure of the amphiphilicity of a helix. *Nature.* 299:371–374.

Engelman, D. M., T. A. Steitz, and A. Goldman. 1986. Identifying nonpolar transbilayer helices in amino acid sequences of membrane proteins. *Annu. Rev. Biophys. Biophys. Chem.* 15:321–353.

Fringeli, U. P., P. Leutert, H. Thurnhofer, M. Fingeli, and M. M. Burger. 1986. Structure-activity relationship in vinculin: an IR/attenuated total reflection spectroscopic and film balance study. *Proc. Natl. Acad. Sci. USA.* 83:1315–1319.

Garnier, J., D. J. Osguthorpe, and B. Robson. 1978. Analysis of the accuracy and implications of simple methods for predicting the secondary structure of globular proteins. *J. Mol. Biol.* 120:97–120.

Geiger, B., and D. Ginsberg. 1991. The cytoplasmic domain of adherens-type junctions. *Cell Mot. Cytoskeleton.* 20:1–6.

Geiger, B., K. T. Tokuyasu, A. H. Dutton, and S. J. Singer. 1980. Vinculin, an intracellular protein localized at specialized sites where microfilament bundles terminate at cell membranes. *Proc. Natl. Acad. Sci. USA.* 77:4127–4131.

Gibrat, J. F., J. Garnier, and B. Robson. 1987. Further developments of protein secondary structure prediction using information theory: new parameters and consideration of residue pairs. *J. Mol. Biol.* 198: 425–443.

Gilmore, A. P., P. Jackson, G. T. Waites, and D. R. Critchley. 1992. Further characterization of the talin binding site in the cytoskeletal protein vinculin. *J. Cell Sci.* 103:719–731.

Gilmore, A. P., C. Wood, V. Ohanian, P. Jackson, B. Patel, D. J. G. Rees, R. O. Hynes, and D. R. Critchley. 1993. The cytoskeletal protein talin contains two distinct vinculin binding domains. *J. Cell Biol.* 122: 337–347.

Glenney, J. R., and L. Zokas. 1989. Novel tyrosine kinase substrates from Rous sarcoma virus-transformed cells are present in the membrane skeleton. *J. Cell Biol.* 108:2401–2408.

Goldmann, W. H., A. Bremer, M. Häner, U. Aebi, and G. Isenberg. 1994. Native talin is a dumbbell-shaped homodimer when it interacts with actin. *J. Struct. Biol.* 112:3–10.

Goldmann, W. H., and G. Isenberg. 1991. Kinetic determination of talin-actin binding. *Biochem. Biophys. Res. Commun.* 178:718–723.

Goldmann, W. H., J. Käs, and G. Isenberg. 1993. Talin decreases the bending modulus of actin filaments. *Biochem. Soc. Trans.* 22:46S.

Goldmann, W. H., V. Niggli, S. Kaufmann, and G. Isenberg. 1992. Probing actin and liposome interaction of talin and talin-vinculin complexes: a kinetic, thermodynamic and lipid labeling study. *Biochemistry.* 31: 7665–7671.

Götter, R., W. H. Goldmann, and G. Isenberg. 1995. Internal actin filament dynamics in the presence of vinculin: a dynamic light scattering study. *FEBS Lett.* 359:220–222.

Hazelrig, J. B., M. K. Jones, and J. P. Segrest. 1993. A mathematically defined motif for the radial distribution of charged residues on apolipoprotein amphipathic α-helices. *Biophys. J.* 64:1827–1832.

Heise, H., T. Bayerl, G. Isenberg, and E. Sackmann. 1991. Human platelet P-235, a talin-like actin binding protein, binds selectively to mixed lipid bilayers. *Biochim. Biophys. Acta.* 1061:121–131.

Horwitz, A., K. Duggan, C. Buck, M. C. Beckerle, and K. Burridge. 1986. Interaction of plasma membrane fibronectin receptor with talin a transmembrane linkage. *Nature.* 320:531–533.

Hunziker, W., M. Spiess, G. Semenza, and H. F. Lodish. 1986. The sucrase-isomaltase complex: primary structure, membrane-orientation and evolution of a stalked, intrinsic brush border protein. *Cell.* 46: 227–234.

Isenberg, G. 1991. Actin binding proteins-lipid interactions. *J. Muscle Res. Cell Motil.* 12:136–144.

Isenberg, G., and W. H. Goldmann. 1992. Actin membrane coupling: a role for talin. *J. Muscle Res. Cell Motil.* 13:587–589.

Isenberg, G., and W. H. Goldmann. 1995. Actin binding proteins-lipid interactions. *In* The Cytoskeleton, Vol. 1. Structure and Assembly. J. E. Hesketh and I. Pryme, editors, JAI Press, Greenwich, CT. 169–204.

Ito, S., D. K. Werth, N. D. Richert, and I. Pastan. 1983. Vinculin phosphorylation by the *src*-kinase. *J. Biol. Chem.* 258:14626–14631.

Jacobs, R. E., and S. H. White. 1989. The nature of the hydrophobic binding of small peptides at the bilayer interface: implication for the insertion of transbilayer helices. *Biochemistry.* 28:3421–3437.

Jennings, M. L. 1989. Topography of membrane proteins. *Annu. Rev. Biochem.* 58:999–1027.

Jockusch, B. M., and G. Isenberg. 1981. Interaction of α-actinin and vinculin with actin: opposite effects on filament network formation. *Proc. Natl. Acad. Sci. USA.* 78:3005–3009.

Johnson, R. P., and S. W. Craig. 1992. Assignment of a phospholipid binding site to the C-terminal tail domain of vinculin. *Mol. Biol. Cell.* 3:266a.

Johnson, R. P., and S. W. Craig. 1994. An intramolecular association between the head and tail domains of vinculin modulates talin binding. *J. Biol. Chem.* 269:12611–12619.

Johnson, R. P., and S. W. Craig. 1995. F-actin binding site masked by the intramolecular association of vinculin head and tail domains. *Nature.* 373:261–264.

Jones, P., P. Jackson, G. J. Price, B. Patel, V. Ohanion, A. L. Lear, and D. R. Critchley. 1989. Identification of a talin binding site in the cytoskeletal protein vinculin. *J. Cell Biol.* 109:2917–2927.

Kaufmann, S., J. Käs, W. H. Goldmann, E. Sackmann, and G. Isenberg. 1992. Talin anchors and nucleates actin filaments at lipid membranes: a direct demonstration. *FEBS Lett.* 314:203–205.

Kaufmann, S., T. Piekenbrock, W. H. Goldmann, M. Bärmann, and G. Isenberg. 1991. Talin binds to actin and promotes filament nucleation. *FEBS Lett.* 284:187–191.

Kreitmeyer, M., G. Gerisch, C. Heizer, and A. Müller-Taubenberger. 1995. A talin homologue of *Dictyostelium* rapidly assembles at the leading edge of cells in response to chemoattractant. *J. Cell Biol.* 129:173–188.

Kroemker, M., A. H. Rüdiger, B. M. Jockusch, and M. Rüdiger. 1994. Intramolecular interactions in vinculin control α-actinin binding to the vinculin head. *FEBS Lett.* 355:259–262.

Kyte, J., and R. F. Doolittle. 1982. A simple method for displaying the hydropathic character of a protein. *J. Mol. Biol.* 157:105–132.

Levin, J. M., and J. Garnier. 1988. Improvements in a secondary structure prediction method based on a search for local sequence homologies and its use as a model building tool. *Biochem. Biophys. Acta.* 955:283–295.

Li, S. C., and C. M. Deber. 1994. A measure of helical propensity for amino acids in membrane environments. *Struct. Biol.* 1:368–373.

Lupas, A., M. VanDyke, and J. Stock. 1991. Predicting coiled coils from protein sequences. *Science.* 252:1162–1164.

Maher, P. A., E. B. Pasquale, J. Y. J. Wang, and S. J. Singer. 1985. Phosphotyrosine-containing proteins are concentrated in focal adhesions and intercellular junctions in normal cells. *Proc. Natl. Acad. Sci. USA.* 82:6576–6780.

Matsuzaki, F., S. Matsumoto, I. Yahara, N. Yonezawa, E. Nishida, and H. Sakai. 1988. Cloning and characterization of porcine brain cofilin cDNA: cofilin contains the nuclear transport signal sequence. *J. Biol. Chem.* 263:11564–11568.

Mclachlan, A. D., M. Stewart, R. O. Hynes, and J. D. G. Rees. 1994. Analysis of repeated motifs in the talin rod. *J. Mol. Biol.* 235: 1278–1290.

Menkel, A. R., M. Kroemker, P. Bubeck, M. Ronsiek, G. Nikolai, and B. M. Jockusch. 1994. Characterization of an F-actin-binding domain in the cytoskeletal protein. *J. Cell Biol.* 126:1231–1240.

Merlie, J. P., D. Fagan, J. Mudd, and P. Needleman. 1988. Isolation and characterization of the complementary DNA for sheep seminal vesicle prostaglandin endoperoxide synthase (cyclooxygenase). *J. Biol. Chem.* 263:3550–3553.

Meyer, R. K. 1989. Vinculin-lipid monolayer interactions: a model for focal contact formation. *Eur. J. Cell. Biol.* 50:491–499.

Milam, L. M. 1985. Electron microscopy of rotary shadowed vinculin and vinculin complexes. *J. Mol. Biol.* 184:543–545.

Molony, L., D. McCaslin, J. Abernethy, B. Paschal, and K. Burridge. 1987. Properties of talin from chicken gizzard smooth muscle. *J. Biol. Chem.* 262:7790–7795.

Mrazek, J., and J. Kypr. 1988. Computer program JAMSEK combining statistical and stereochemical rules for the prediction of protein secondary structure. *Cabios.* 4:297–302.

Niggli, V., D. P. Dimitrov, J. Brunner, and M. M. Burger. 1986. Interaction of the cytoskeletal component vinculin with bilayer structures analyzed with a photoactivatible phospholipid. *J. Biol. Chem.* 261:6912–6918.

Niggli, V., S. Kaufmann, W. H. Goldmann, T. Weber, and G. Isenberg. 1994. Identification of functional domains in the cytoskeletal protein talin. *Eur. J. Biochem.* 224:951–957.

Niggli, V., L. Sommer, J. Brunner, and M. M. Burger. 1990. Interaction *in situ* of the cytoskeletal protein vinculin with bilayers studied by introducing a photoactivatible fatty acid into living chicken embryo fibroblasts. *Eur. J. Biochem.* 187:111–117.

Otto, J. J. 1990. Vinculin. *Cell Motil. Cytoskeleton.* 16:1–6.

Pavalko, F., C. Otey, K. O. Simon, and K. Burridge. 1991. α-Actinin: a direct link between actin and integrins. *Biochem. Soc. Trans.* 19: 1065–1069.

Picot, D., and R. M. Garavito. 1994. Prostaglandin H synthase: implications for membrane structure. *FEBS Lett.* 346:21–25.

Price, G. J., P. Jones, M. D. Davison, B. Patel, R. Bendori, B. Geiger, and D. R. Critchley. 1989. Primary sequence and domain structure of chicken vinculin. *Biochem. J.* 259:453–461.

Price, G. J., P. Jones, M. D. Davison, B. Patel, I. C. Eperon, and D. R. Critchley. 1987. Isolation and characterization of a vinculin cDNA from chicken embryo fibroblasts. *Biochem. J.* 245:595–603.

Ptitsyn, O. B., and A. V. Finkelstein. 1983. Theory of protein secondary structure and algorithm of its prediction. *Biopolymers.* 22:15–25.

Rees, D. J. G., S. E. Ades, S. J. Singer, and R. O. Hynes. 1990. Sequence and domain structure of talin. *Nature.* 347:685–689.

Ruddies, R., W. H. Goldmann, G. Isenberg, and E. Sackmann. 1993. The viscoelasticity of entangled actin networks: influence of defects and modulation by talin and vinculin. *Eur. Biophys. J.* 22:309–321.

Samuels, M., R. M. Ezzell, T. J. Cardozo, D. R. Critchley, J-L. Coll, and E. D. Adamson. 1993. Expression of chicken vinculin complements the adhesion-defective phenotype of a mutant mouse F9 embryonal carcinoma cell. *J. Cell Biol.* 121:909–921.

Sefton, B. M., and T. Hunter. 1981. Vinculin: a cytoskeletal target of the transforming protein of Rous sarcoma virus. *Cell.* 24:165–174.

Segrest, J. P., H. DeLoof, J. G. Dohlman, C. G. Brouillette, and G. M. Anantharamaiah. 1990. Amphipathic helix motif: classes and properties. *Proteins Struct. Funct. Genet.* 8:103–117.

Segrest, J. P., M. K. Jones, H. De Loof, C. G. Brouillette, Y. V. Venkatachalapathi, and G. M. Anantharamaiah. 1992. The amphipathic helix in the exchangeable apo-lipoproteins: a review of secondary structure and function. *J. Lipid Res.* 33:141–166.

Simon, K. O., and K. Burridge. 1991. Characterization of the interaction between talin and the cytoplasmic domain of β_1 integrin. *J. Cell Biol.* 115:351a.

Turner, C. E., J. R. Glenney, and K. Burridge. 1990. Paxillin: a new vinculin-binding protein present in focal adhesions. *J. Cell Biol.* 111: 1059–1068.

Wachsstock, D. H., J. A. Wilkins, and S. Lin. 1987. Specific interaction of vinculin with α-actinin. *Biochem. Biophys. Res. Commun.* 146:554–560.

Weller, P. A., E. P. Ogryzko, E. B. Corben, N. I. Zhidkova, B. Patel, G. J. Price, N. K. Spurr, V. E. Koteliansky, and D. R. Critchley. 1990. Complete sequence of human vinculin and assignment of the gene to chromosome 10. *Proc. Natl. Acad. Sci. USA.* 87:5667–5671.

Wood, C. K., C. E. Turner, P. Jackson, and D. R. Critchley. 1994. Characterisation of the paxillin-binding site and the C-terminal focal adhesion targeting sequence in vinculin. *J. Cell Sci.* 107:709–717.

Yamamoto, Y., C. A. Hake, B. M. Martin, K. A. Kretz, A. J. Ahern-Rindell, S. L. Naylor, M. Mudd, and J. S. O'Brien. 1990. Isolation, characterization, and mapping of a human acid β-galactosidase cDNA. *DNA Cell Biol.* 9:119–127.

Yonezawa, N., Y. Homma, I. Yahara, H. Sakai, and E. Nishida. 1991. A short sequence responsible for both phosphoinositide binding and actin binding activities of cofilin. *J. Biol. Chem.* 266:17218–17221.